



Cite this: *Environ. Sci.: Atmos.*, 2022, **2**, 279

Ice nucleating particles in the Canadian High Arctic during the fall of 2018†

Jingwei Yun, ^a Erin Evoy, ^a Soleil E. Worthy, ^a Melody Fraser, ^b Daniel Veber, ^b Andrew Platt, ^b Kevin Rawlings, ^b Sangeeta Sharma, ^b W. Richard Leaitch ^{‡b} and Allan Bertram ^{*a}

Ice nucleating particles (INPs) are a small subset of atmospheric particles that can initiate the formation of ice in clouds, including mixed-phase clouds. Here we report concentrations of INPs during October and November of 2018 at Alert, Nunavut, in the Canadian High Arctic. Our results show that average INP concentrations in October were higher than those in November. Based on an ammonium sulfate assay, mineral dust was an important component of the INP population at temperatures (T) ≤ -21 °C and $T \leq -20$ °C for October and November, respectively. Based on a heat assay, biological particles were an important component of the INP population at $T \geq -21$ °C and $T \geq -16.5$ °C for October and November, respectively. In addition, INP concentrations were correlated with aluminum concentrations (a tracer for mineral dust), possibly suggesting a significant fraction of the mineral dust and biological INPs came from the same source. Particle dispersion modelling and correlations between INP concentrations and aluminum suggest a significant fraction of the INPs came from ice-free and snow-free land at latitudes >50 °N. Since the coverage of ice-free and snow-free land in the Arctic is expected to increase as temperatures increase in the Arctic, these results have important implications for climate feedback mechanisms in the region.

Received 22nd August 2021
Accepted 6th January 2022

DOI: 10.1039/d1ea00068c
rsc.li/esatmospheres

Environmental significance

Ice nucleating particles (INPs) can trigger ice formation in clouds and strongly influence the optical properties and lifetime of clouds. However, the properties of atmospheric INPs are still poorly constrained, especially for the Arctic, a region highly sensitive to global warming. Here we investigate the concentration, composition, and sources of INPs collected at a ground station at Alert, Nunavut, Canada. The results suggest that the main components of INPs include mineral dust and biological particles, and the INPs are likely from the ice-free and snow-free land at latitudes >50 °N.

1. Introduction

Mixed-phase clouds, which contain both liquid and ice, are abundant in the Arctic and play an important role in precipitation and climate in this region.^{1,2} Ice nucleating particles (INPs) are atmospheric aerosol particles that can initiate the formation of ice in clouds, including mixed-phase clouds. These particles can modify the properties of mixed-phase clouds, including their lifetime and optical properties, by changing the ratio of ice to liquid water in these clouds.^{3–8} Hence, information on the concentrations, composition, and sources of INPs in the Arctic is critical to predict climate and the hydrological cycle

in the region. Furthermore, as temperatures increase in the Arctic,^{9,10} the coverage of sea ice and land snow is expected to decrease.¹¹ This decrease in sea ice and land snow may lead to an increase in the INP concentrations in the Arctic atmosphere,^{12–15} leading to a possible increase in precipitation, a decrease in the lifetime of mixed phase clouds, and a positive climate feedback in the region.^{6,16} Knowledge of the concentrations, composition, and sources of INPs in the Arctic is also needed to predict the importance of this climate feedback mechanism.

Several studies have measured the concentrations of INPs in the Arctic.^{16–30} In most cases, these measurements were carried out for relatively short periods of time during intensive field campaigns. A few studies have quantified INP concentrations over longer periods of time.^{17,19–21} Fountain and Ohtake¹⁹ measured INP concentrations at 3 ground sites in Alaska for a full year and showed that the INP concentrations were higher in the summer and lower in the winter. Bigg²⁰ and Bigg and Leck²¹ observed a decline in the INP concentrations over the

^aDepartment of Chemistry, University of British Columbia, Vancouver, BC, V6T 1Z1, Canada. E-mail: bertram@chem.ubc.ca

^bClimate Research Division, Environment and Climate Change Canada, Toronto, ON, M3H 5T4, Canada

† Electronic supplementary information (ESI) available. See DOI: [10.1039/d1ea00068c](https://doi.org/10.1039/d1ea00068c)

‡ W. Richard Leaitch is retired.



Arctic Ocean from the summer to the fall. In addition, Wex *et al.*¹⁷ recently monitored INP concentrations at 4 stations in the Arctic and observed a seasonal variation in the concentrations of INPs with higher concentrations in the summer and fall and lower concentrations in the winter and spring. Continued measurements of the concentrations of INPs in the Arctic are necessary to improve our understanding of the concentrations of INPs in the region and how these concentrations vary with freezing temperature, season, and location in the Arctic.

Compared to studies that measured the concentrations of INPs in the Arctic, fewer studies have directly probed the composition of INPs in the Arctic. Several of the studies that directly probed the composition of INPs in the Arctic identified mineral dust as a significant contributor of INPs in the region. As an example, Kumai and Francis³² characterized residuals of natural snow crystals forming in a cloud at -20 to -5 °C over Greenland in the summer using electron microscopy and concluded that the snow crystals were formed mainly on clay mineral particles. Using transmission electron spectroscopy and energy dispersive X-ray analysis (TEM-EDX), Rogers *et al.*³¹ showed that INPs over the Arctic Ocean during the late spring consisted of crustal minerals (16%) and carbonaceous particles (76%) for freezing temperatures ranging from -25 to -20 °C. Similarly, using TEM-EDX, Prenni *et al.*²² showed that INPs over northern Alaska in October often consisted of metal oxides or mineral dust and carbonaceous particles for freezing temperatures from -28 to -6 °C.

Some studies that probed the composition of INPs in the Arctic identified biological particles as a significant contributor to INP concentrations in the region. Using a heat treatment assay, Šantl-Temkiv *et al.*²⁷ showed that 82% to 100% of the INPs at $T \geq -15$ °C over Greenland during the summer were likely biological. Also using a heat treatment assay, Hartmann and Adachi *et al.*²⁸ and Hartmann and Gong *et al.*²⁹ showed that for some of their samples collected over the Arctic Ocean during the spring and early summer, 100% of the INPs at $T \geq -15$ °C were likely biological. In addition, other researchers have speculated that biological particles were an important source of INPs in the Arctic based on the warm freezing temperatures ($T \geq -15$ °C) of their samples.^{17,18,23,30} Despite these measurements, more work is still needed to better understand the composition of INPs in the Arctic. For example, more information is needed on the relative contributions of mineral dust particles and biological particles to the INP population and how the relative contributions change with the freezing temperature, season, and location in the Arctic. In addition, non-proteinaceous organics may play an important role in ice nucleation in the atmosphere.^{33,34} Studies that determine the relative importance of non-proteinaceous organics are also needed.

Sources of INPs in the Arctic have been discussed in some previous studies. Some studies suggested local sources of INPs during the spring and summer. Possible local sources included the open ocean, snow-free land, open leads, and polynyas.^{17,18,26-28} Besides local sources, long range transport from mid-latitudes has also been suggested as an important

source of the INPs in the Arctic.^{22,24} Despite these studies, additional studies of the source regions of INPs in the Arctic are needed since the source regions might change with the sampling site, season, and freezing temperature range.

In the following, we investigated the concentration of INPs in the immersion freezing mode during October and November at Alert, Nunavut, in the Canadian High Arctic. Immersion freezing refers to ice nucleation on INPs immersed in liquid droplets. This mode of heterogeneous freezing has been shown to be a dominant mode of ice nucleation in mixed-phase clouds.^{35,36} In addition to measuring the concentrations of INPs, we probed the composition of the INPs by monitoring the changes in the INP concentrations after exposing the samples to ammonium sulfate (an ammonium sulfate assay) and heating at 100 °C (a heat assay). The ammonium sulfate assay, which has not been used previously in field studies, was used to explore the importance of mineral dust INPs in the samples. The heat assay was used to detect biological INPs in the samples. We also investigated correlations between the concentrations of INPs and concentrations of Al, Na⁺, and Cl⁻ to provide complementary information on the composition of aerosols that may act as INPs. We also used a Lagrangian particle dispersion model to provide information on the source regions of the INPs.

2. Experimental method

2.1. Sampling site and aerosol sampling

Sampling was performed daily at the Dr Neil Trivett Global Atmosphere Watch Observatory, Alert, Nunavut, Canada (82.5 °N, 62.5 °W) from October 19th to November 17th, 2018. The observatory is operated by Environment and Climate Change Canada and located on a plateau with an altitude of 185 m and 6 km from the Canadian Forces Station Alert. The population of the Canadian Forces Station was reported as 62 in 2016. The closest town is Grise Fiord, which is located 800 km to the south of Alert and has a population of 129. The meteorological variables during sampling are indicated in Fig. S1.† During the sampling campaign, the precipitation was low, and the ambient temperature ranged from -35 °C to -10 °C (with an average of -20.8 °C). The relative humidity (with respect to water) usually stayed above 75% (with an average of 80.8%), and the wind mainly came from southwest and northwest with the speed below 15 km h⁻¹.

For INP measurements, aerosol particles were sampled through a louvered total suspended particulate (TSP) inlet connected to an insulated and vertically oriented stainless tube (10 cm diameter). The losses of particles from 20 nm to 1 μ m and probably up to 5 μ m were small, if not negligible through the sampling inlet and tubing.³⁷ Aerosols were collected with 47 mm diameter nucleopore membrane filters (GE Healthcare Whatman™), which were placed in an in-line aluminum filter holder. The collection time for these samples ranged from 17 to 24 hours, with a flow rate of 12 L min⁻¹. The membrane filters had a pore size of 0.2 μ m and a high collection efficiency of aerosol particles (>80% with the lowest collection efficiency at diameters of 0.1 μ m).^{38,39} This type of



filter was used previously for INP collection.³⁹ After collection, the membrane filters were stored in 50 mL polypropylene tubes (Corning™ Falcon) in a fridge at approximately 4 °C until analyzed (Section 2.2).

For the measurements of Al, Na⁺, and Cl⁻, 47 mm diameter Teflon filters (PT 47 Filter, Measurement Technology Laboratories) were used to collect aerosol samples daily with a pore size of 2 µm at a flow rate of 16.7 L min⁻¹ for 17–24 hours for the same sampling period and at the same sampling site as the INP samples. This type of Teflon filter has a collection efficiency of higher than 99.99% for particles ≥ 0.1 µm based on the manufacturer's specifications. After collection, the Teflon filters were stored in Petri slides in a fridge at approximately 4 °C until analyzed (Section 2.6).

2.2. INP measurements for samples without any treatment

The nucleopore membrane filters collected at Alert were analyzed for INPs at the University of British Columbia. To extract the aerosols from the filters, 5 mL of ultra-pure water (distilled water purified by Millipore system with a resistivity of 18.2 MΩ at 25 °C) was added to the polypropylene tubes containing the filters and then the tubes were shaken for one hour with an orbital shaker at 200 rpm. The INP concentration in each suspension was then determined using the droplet freezing technique as described previously.^{40–42} For each sample, 60 1 µL droplets of the suspension were pipetted onto hydrophobic siliconized glass slides (Hampton Research) located on a cold plate (Grant EF5600). Another 60 1 µL droplets of Milli-Q water were pipetted onto the previous droplets, resulting in a final volume of 2 µL per droplet. The second 1 µL droplets were added to give the same final volume as the droplets used in the ammonium sulfate assay (see below for additional details). The droplets were then isolated from the surrounding atmosphere with a transparent chamber with a digital camera located on the top of the chamber. To prevent condensation of water vapor on the slides during cooling, a small flow of dry N₂ was passed through the chamber. The temperature of the cold plate was first set to 20 °C, then decreased to -2 °C at a rate of 10 °C min⁻¹, stabilized for 1 minute, and then cooled at a rate of 3 °C min⁻¹ until all the droplets froze. Droplet freezing was recorded by the digital camera and the video was analyzed either manually or automatically by a MATLAB script to determine the freezing temperature of each droplet. The freezing temperatures were determined based on the brightness of the droplets. For autonomous detection, the freezing temperature was assigned as the temperature when the first derivative of the brightness reached a maximum.⁴³ The uncertainty in the freezing temperature was ± 0.25 °C based on specifications from the manufacturer.

After determining the freezing temperature of each droplet, the INP concentration in the air was calculated with the following equation.⁴⁴

$$N_{\text{INPs}}(T) = \frac{-\ln\left(\frac{N_u}{N_0}\right) V_{\text{suspension}} \times 2}{V_{\text{droplet}} V_{\text{air}}}, \quad (1)$$

where $N_{\text{INPs}}(T)$ is the number of INPs per volume of the air at temperature T , N_u is the number of unfrozen droplets, N_0 is the number of total droplets, $V_{\text{suspension}}$ is the volume of water (5 mL) used to generate the suspensions containing INPs from the filters, V_{droplet} is the final volume of the droplets (2 µL) used in the freezing experiments, and V_{air} is the volume of sampled air for each filter (Table S5†). The factor of 2 in eqn (1) was included since the 1 µL droplets generated from the suspensions were each diluted with a second 1 µL droplet containing only Milli-Q water. The uncertainty in $N_{\text{INPs}}(T)$ was $\pm 98\%$ at the lowest N_u/N_0 value (1/60) and $\pm 22\%$ at the highest N_u/N_0 value (59/60) used in our experiments based on nucleation statistics.⁴⁵

2.3. Ammonium sulfate assay

An ammonium sulfate assay was used as an indicator for the presence of mineral dust INPs in the samples, as suggested previously.^{46,47} This assay, which has not been used previously for field studies, is based on laboratory studies of mineral dust and non-mineral dust INPs in the presence of dilute ammonium sulfate solutions. Several previous studies have shown that the ice nucleation ability of many types of mineral dusts (feldspars, kaolinite, montmorillonite, micas, and quartz) but not all (amorphous silica and gibbsite) increases in the presence of dilute ammonium sulfate solutions (<0.1 M) after correction for freezing point depression by the salts.^{46–51} See Table S1† for a summary of these previous studies. The reason why ammonium sulfate improves the ice nucleating ability of many types of mineral dust likely involves ion exchange of NH₄⁺ with parent cations at the mineral dust surface or adsorption of NH₄⁺ at the mineral dust surface.^{46,48,49} Both processes could affect the orientation of water molecules at the mineral dust surface and, hence, ice nucleation.

On the other hand, previous studies have shown that the ice nucleation ability of many non-mineral dust aerosols typically found in the atmosphere (bacteria, fungi, sea-ice diatom exudates, sea-surface microlayer samples, humic substances, and leaf derived INPs) either decrease or are not affected by the presence of dilute ammonium sulfate solutions (<0.1 M), after correction for freezing point depression by the salt.^{46,47,52} See Table S2† for a summary of previous work with non-mineral aerosol particles. Consistent with these previous studies, we assumed that an increase in the ice nucleation ability of a sample after the addition of ammonium sulfate at a concentration of 0.05 M and after correction for freezing point depression by the salt indicates the presence of mineral dust INPs. We also note that Reischel and Vali (1975) observed that ammonium salts increased the ice nucleating ability of AgI and CuS hydrosols (two non-mineral dusts) but aerosols containing AgI and CuS are not expected to be abundant in the Arctic atmosphere.^{53,54}

For the ammonium sulfate assay, we first pipetted 60 droplets of the suspensions containing the INPs onto hydrophobic glass slides located on the cold stage. Then a second droplet containing 0.1 M ammonium sulfate was added to each of the previous droplets, resulting in each droplet having a volume of 2 µL and an ammonium sulfate concentration of 0.05 M. The



freezing temperatures of these droplets were then measured and corrected for freezing point depression by ammonium sulfate as described below. The INP concentrations were determined with eqn (1) and compared to the INP concentrations determined for the case without ammonium sulfate. We assume that a significant increase in the INP concentration indicates that the samples likely contain mineral dust INPs.

The freezing point depression caused by the addition of ammonium sulfate (0.05 M) was determined with the following equation.⁵⁵

$$\Delta T_f = K_f \times m \times i \quad (2)$$

where ΔT_f is the estimated freezing point depression, K_f is the freezing point depression constant ($1.86 \text{ }^{\circ}\text{C mol}^{-1} \text{ kg}$), m is the molality of the solutes (0.05 mol kg^{-1} in this case), and i is the van't Hoff factor (3 for ammonium sulfate). Based on eqn (2), the freezing point depression was $0.28 \text{ }^{\circ}\text{C}$, and all freezing temperatures for droplets with 0.05 M ammonium sulfate were corrected by this amount.

2.4. Heat assay

Previous studies have shown that proteinaceous INPs can undergo denaturation and lose their ice nucleating ability after undergoing heat treatment at temperatures from $60 \text{ }^{\circ}\text{C}$ to $105 \text{ }^{\circ}\text{C}$.^{56–60} As a result, heating tests have been used in previous studies as a tool to identify possible biological INPs.^{27–29,33,34,41,56,61,62} Consistent with previous studies, we assume that a decrease in the INP concentrations of the samples after heating indicates the presence of biological INPs, similar to previous studies in the Arctic.^{27–29}

For the heating assay, an aliquot of each suspension generated from the filter samples was placed in a polypropylene tube capped with a lid and heated at $100 \text{ }^{\circ}\text{C}$,^{41,42} for one hour in a heating block (AccuBlock, Labnet). The freezing temperatures and INP concentrations of the heated samples were then determined as described in Section 2.2.

2.5. Negative controls for the freezing experiments

We used Milli-Q water (5 trials) and a 0.05 M ammonium sulfate solution (3 trials) as negative controls. 5 mL of Milli-Q water or the ammonium sulfate solution was added to polypropylene tubes containing new membrane filters and the tubes were then shaken for one hour with an orbital shaker at 200 rpm. The resulting solution was then used in the freezing experiments as described in Section 2.2. The results from these freezing experiments were then used to calculate an average fraction frozen curve for the negative controls (the black curve in Fig. S2†). Eqn (1) was then used to calculate the average INP concentration for the negative controls, assuming the volume of sampled air for the negative controls was the same as the volume of sampled air for the aerosol samples. The average INP concentration for the negative controls was subtracted from the measured INP concentrations for each sample.

In this paper, we only report the INP concentrations at $T \geq -22 \text{ }^{\circ}\text{C}$. We focus on this temperature range because, in some cases, all droplets froze when $T \geq -22 \text{ }^{\circ}\text{C}$ (Fig. S3†). In these cases, the concentration of INPs could not be calculated from eqn (1). For $T \geq -22 \text{ }^{\circ}\text{C}$, the fraction of droplets that froze for the negative controls on average was $\leq 5\%$ (Fig. S3†).

2.6. Measurements of the concentrations of Al, Na^+ , and Cl^-

The Teflon filters collected at Alert were analyzed to determine the concentrations of Al, Na^+ , and Cl^- for the same sampling times as the INP samples. The filters were analyzed at Chester LabNet, Oregon, USA. One set of filters was used to determine the concentration of the element Al by inductively coupled plasma atomic emission spectroscopy (ICP-AES). The element Al is a major constituent of the Earth's crust⁶³ and has been used in the past as a tracer of mineral dust in the atmosphere.^{53,64–66} The other set of filters was used to determine the concentration of Na^+ and Cl^- by ion chromatography (IC). These ions are major constituents of sea salts and have been used as a tracer of sea spray aerosol in the past.^{64–67}

For ICP-AES analysis, the Teflon filters were digested in a heated ultrasonic bath after the addition of concentrated nitric and hydrochloric acids. The resulting solutions were then atomized into an argon plasma and the element Al was identified by a characteristic emission line. For IC analysis, the Teflon filters were immersed in 10 mL of deionized water and sonicated for 60 minutes. Concentrations of soluble ions were then determined by ion chromatography (Thermo Scientific ICS-500), following the United States Environmental Protection Agency (USEPA) methods 300.0 and 300.7.^{68,69} Briefly, the extracted solution was injected into an ion exchange column operating under high pressure, and the ions were separated by the ion exchange column and detected by conductivity of the post-column eluent.

2.7. Particle dispersion modelling

To help determine possible sources of INPs in the samples, the FLEXible PARTICle dispersion model (FLEXPART)⁷⁰ was used in the backward mode. The model was driven by the National Centers for Environmental Prediction (NCEP) Final (FNL) Operational Global Analysis Data. In each simulation, 100 000 particles were released at the sampling site ($82.5 \text{ }^{\circ}\text{N}, 62.5 \text{ }^{\circ}\text{W}$) within one minute and followed backward for 7 days with outputs generated at 1 hour intervals. Wet deposition was not considered here when calculating the back trajectories of the particles. For each INP sample collected at Alert, a simulation was run every three hours during the sampling period. The outputs from all the simulations were then averaged to generate a potential emission sensitivity (PES) plot for each sample. Since we wanted to identify possible sources of the INPs, which most likely originated from the Earth's surface, we only used data from the surface to 100 meters above the surface resulting in near-surface PES plots (*i.e.*, footprint PES plots).



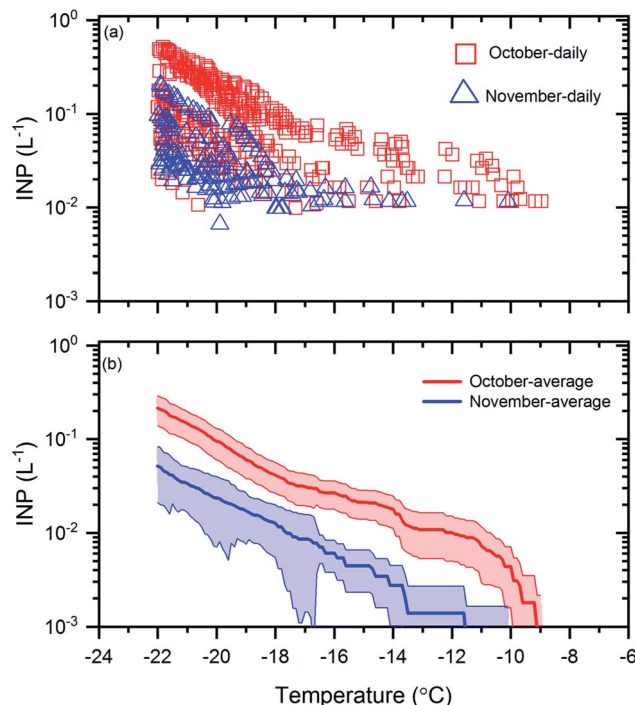


Fig. 1 INP concentrations during October and November. Panel (a): the INP concentrations measured as a function of temperature for the daily samples collected in October and November. Uncertainties are not shown for clarity. Panel (b): the monthly average INP concentrations as a function of temperature for the samples collected in October and November. The shaded regions in panel (b) represent the 83% confidence bands of the monthly average INP concentrations. Two data sets with normal distributions are statistically different at a confidence level of 95% if their 83% confidence bands of the means do not overlap.⁷¹

3. Results and discussion

3.1. The concentrations of INPs measured at Alert

Shown in Fig. 1a are the measured INP concentrations as a function of temperature for all 30 samples. The lower detection limit for the INP measurements was approximately 0.01 L^{-1} for each sample. Within the temperature range investigated ($\geq -22\text{ }^\circ\text{C}$), the measured INP concentrations for the October samples varied from 0.01 L^{-1} to 0.5 L^{-1} and the measured INP concentrations for the November samples varied from 0.01 L^{-1} to 0.2 L^{-1} . The largest variation of INP concentrations between daily samples occurred at $-22\text{ }^\circ\text{C}$, with a factor of ~ 20 for the October samples and a factor of ~ 8 for the November samples.

To determine if the mean INP concentrations for October were significantly different from November at the 95% confidence level, in Fig. 1b, we compared the mean INP concentrations with 83% confidence bands for the October and November samples. Two data sets are statistically different at the 95% confidence level if their 83% confidence bands of the means do not overlap.⁷¹ Note, to determine if two datasets are significantly different at the 95% confidence level, the 83% confidence bands, rather than the 95% confidence bands, should be used, as shown previously.⁷¹ Based on Fig. 1b, the average INP concentrations during October were a factor of 3 to 6 higher

than November and the differences were statistically significant.

The freezing temperature at which 50% of the droplets froze in an experiment (T_{50}) is often used to compare freezing efficiencies. In Fig. S4,[†] we compared the mean T_{50} values for the October and November samples. Based on Fig. S4,[†] the mean T_{50} values for October were $1.9\text{ }^\circ\text{C}$ warmer than November and the differences were statistically significant at the 95% confidence level.

Fig. 2 shows a comparison of the INP concentrations measured in our study with the INP concentrations measured in previous ground-based or ship-based INP measurements in the Arctic (the locations of previous field measurements are given in Table S3[†]). The average daily INP concentrations at $-16\text{ }^\circ\text{C}$ and $-22\text{ }^\circ\text{C}$ in our study were 0.04 L^{-1} and 0.22 L^{-1} , respectively, for the October samples, and 0.013 L^{-1} and 0.052 L^{-1} , respectively, for the November samples. These values were within the concentration range of the previous studies.^{17-21,23-27,30,72}

Also included in Fig. 2 (shaded region) is the range of INP concentrations measured from precipitation and cloud water samples mainly collected over mid-latitudes in North America and Europe.⁷³ Based on Fig. 2, at $T \geq -16\text{ }^\circ\text{C}$, the INP concentrations measured at the surface in the Arctic are mostly consistent with the concentration range reported by Petters and Wright.⁷³ However, at $T \leq -16\text{ }^\circ\text{C}$, the INP concentrations

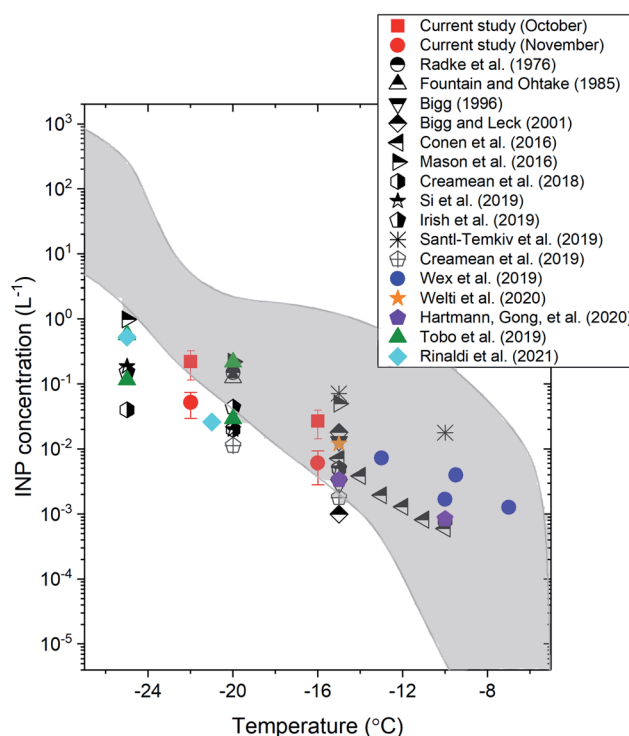


Fig. 2 The average INP concentrations as a function of temperature in the Arctic measured in the current study and in previous ground-based or ship-based studies. The sampling platform, location, and time of each study are indicated in Table S3.[†] The error bars for the current study correspond to the 95% confidence intervals of the means. The region shaded in grey shows the literature data from ref. 73 for precipitation and cloud water samples.



measured at the surface in the Arctic are often less than the concentration range reported by Petters and Wright.⁷³ These results suggest that INP concentrations at the surface in the Arctic may often be lower than those in mid-latitude continental areas at $T \leq -16$ °C, consistent with the conclusion of Wex *et al.*¹⁷ using a similar analysis.

3.2. Results based on the ammonium sulfate assay

To determine if mineral dust particles are an important component of the INP population, we compared the INP concentrations before and after exposure to a 0.05 M ammonium sulfate solution (see Section 2.3). An increase in the INP concentrations after exposure to ammonium sulfate suggests the presence of mineral dust INPs. Shown in Fig. 3 are results for the October samples (Fig. 3a and b) and the November samples (Fig. 3c and d) before and after ammonium sulfate treatment.

For the October samples, the average INP concentrations after ammonium sulfate treatment were statistically higher (95% confidence level) than those before ammonium sulfate

treatment for $T \leq -21$ °C (Fig. 3b). For the November samples, the average INP concentrations after ammonium sulfate treatment were statistically higher (95% confidence level) than those before ammonium sulfate treatment for $T \leq -20$ °C (Fig. 3d). These results suggest that mineral dust is a significant component of the INP population for October and November at $T \leq -21$ °C and $T \leq -20$ °C, respectively. These findings are consistent with the previous studies that have identified mineral dust as an important component of the INP population at temperatures of -28 °C to -6 °C in the Arctic.^{22,31}

3.3. Results based on the heat assay

To determine if biological INPs were an important component of the INP population, we determined the change in the INP concentrations after heating the samples at 100 °C (see Section 2.4). A decrease in the INP concentrations was assumed to indicate the presence of biological INPs. Shown in Fig. 4 are results for the October samples (Fig. 4a and b) and the November samples (Fig. 4c and d) before and after heat treatment.

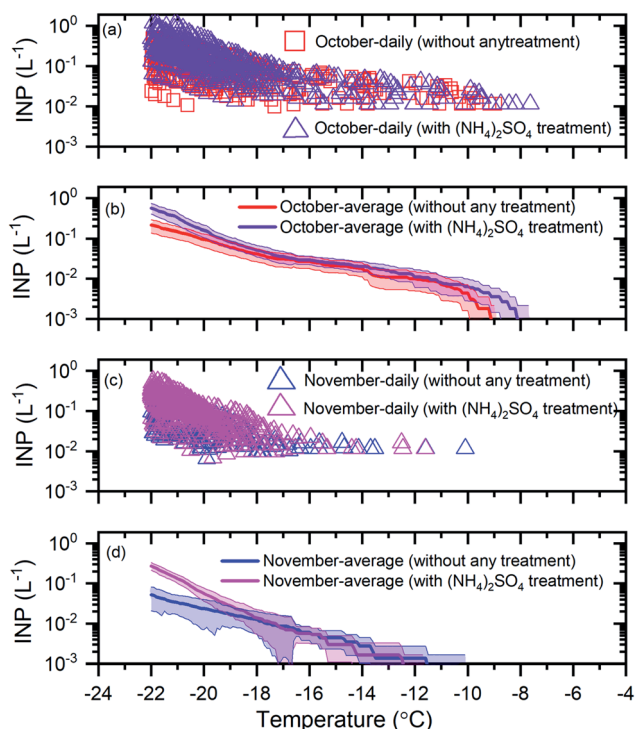


Fig. 3 The effect of ammonium sulfate treatment on the INP concentrations. Panel (a): the daily INP concentrations measured in October without any treatment and with ammonium sulfate treatment. Uncertainties are not shown for clarity. Panel (b): the monthly average INP concentrations for October without any treatment and with ammonium sulfate treatment. Panel (c): the daily INP concentrations in November without any treatment and with ammonium sulfate treatment. Uncertainties are not shown for clarity. Panel (d): the monthly average INP concentrations for November without any treatment and with ammonium sulfate treatment. The shaded regions in panel (b) and panel (d) indicate 83% confidence bands. Two data sets with normal distributions are statistically different at a confidence level of 95% if their 83% confidence bands of the means do not overlap.⁷¹

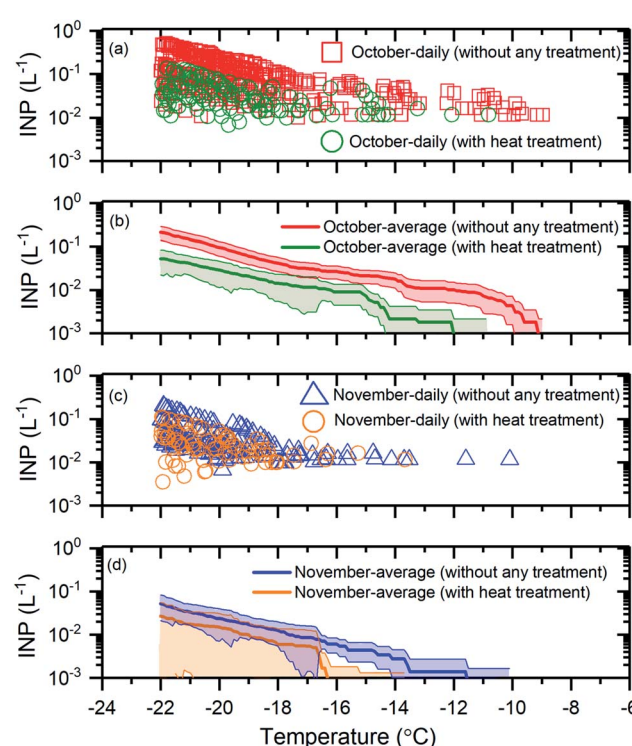


Fig. 4 The effect of heat treatment on the INP concentrations. Panel (a): the daily INP concentrations measured in October without any treatment and with heat treatment. Uncertainties are not shown for clarity. Panel (b): the monthly average INP concentrations for October without any treatment and with heat treatment. Panel (c): the daily INP concentrations in November without any treatment and with heat treatment. Uncertainties are not shown for clarity. Panel (d): the monthly average INP concentrations for November without any treatment and with heat treatment. The shaded regions in panel (b) and panel (d) indicate 83% confidence bands. Two data sets with normal distributions are statistically different at a confidence level of 95% if their 83% confidence bands of the means do not overlap.⁷¹



For the October samples, the average INP concentrations after heat treatment were statistically lower (95% confidence level), at $T \geq -20$ °C (Fig. 4b). For the November samples, the average INP concentrations after heat treatment were statistically lower (95% confidence level) at $T \geq -16.5$ °C (Fig. 4d). These results suggest that a large fraction of the INPs were likely biological for the October and November samples at $T \geq -21$ °C and $T \geq -16.5$ °C, respectively. The findings based on the heat assay are consistent with previous studies that have shown biological particles as an important component of the INP population for certain times of the year at freezing temperatures ≥ -15 °C in the Arctic based on a similar heat treatment assay.²⁷⁻²⁹

Overall, our results provide additional evidence that biological INPs likely make up a significant fraction of the INP population in the Arctic at freezing temperatures ≥ -15 °C and even lower temperatures for certain times of the year.

3.4. Correlations between the concentrations of INPs and Al, Na^+ , and Cl^-

In addition to measuring the concentrations of INPs, we measured the concentrations of tracer chemical species for mineral dust and sea spray aerosol. Al was used as a tracer for mineral dust,^{53,64-66} and Na^+ and Cl^- were used as tracers for sea spray aerosols.⁶⁴⁻⁶⁷

The concentration of Al was correlated ($R = 0.72$) with the INP concentrations at -22 °C, and the correlation was statistically significant ($p < 0.05$) (Table 1). This is consistent with our finding that a significant fraction of the INP population at -22 °C contained mineral dust particles based on the ammonium sulfate assay (see Section 3.2). At -16 °C, the correlation coefficient was smaller ($R = 0.58$) but still statistically significant ($p < 0.05$). However, the ammonium sulfate assay did not indicate that mineral dust particles were an important component of the INP population at this freezing temperature. One possible explanation for this apparent discrepancy is that the biological INPs, which were important at the warmer temperatures, and the mineral dust INPs, which were important at lower temperatures in our samples, came from the same sources in some cases. Consistent with this explanation, previous studies have shown that aerosol particles from soil dust contain both biological and mineral dust

INPs.^{33,62,74,75} In contrast to Al, the correlation coefficients between concentrations of Na^+ and Cl^- and INP concentrations at freezing temperatures of -22 °C and -16 °C were small (≤ 0.25) and not statistically significant ($p > 0.05$).

3.5. Results from particle dispersion modelling

To provide information on the source regions of the INPs in our study, we calculated footprint PES plots for each sample using FLEXPART run in the backward mode. The footprint PES plots show the residence time of particles in the layer from 0 to 100 m in altitude during the previous 7 days. Fig. 5 shows the average footprint PES plot for all 30 samples (Fig. 5a), the average footprint PES plot for the October samples (Fig. 5b), and the average footprint PES plot for the November samples (Fig. 5c). Based on Fig. 5a-c, the source regions of the INPs were likely at latitudes >50 °N. In addition, the footprint PES plots for October are similar to those for November, although the footprint PES plots for October tend to have higher residence time over Northern Canada and Asian Arctic compared to those for November.

Shown in Fig. 5d-f are maps of the surface coverage types for October 19th, November 3rd, and November 17th, which correspond to the start, midway point, and end of the sampling period, respectively. During the field campaign, the snow coverage and sea-ice coverage largely increased, while the bare (*i.e.*, ice-free and snow-free) land and open ocean significantly decreased for latitudes >50 °N (Fig. 5d-f). The footprint PES plots for each sample were combined with daily maps of surface coverage types (similar to Fig. 5d-f) to determine the total residence time that each air mass sampled spent in the footprint layer over a specific surface type (Table S4†). At freezing temperatures of -22 °C and -16 °C, statistically significant positive correlations ($R = 0.53$ and 0.49 , respectively) were observed between the INP concentrations and the residence time in the footprint layer over bare land (Table 2). On the other hand, at the same freezing temperatures, statistically significant negative correlations ($R = -0.42$ and -0.39 , respectively) were observed between the INP concentrations and the residence time in the footprint layer over sea ice (Table 2). In addition, no statistically significant correlations were observed between the INP concentrations and the residence time in the footprint layer over open ocean and land snow (Table 2).

The results of particle dispersion modelling and the positive correlation between INP concentrations and Al suggest that the INPs were mostly from bare land at latitudes >50 °N. In the current study, higher average INP concentrations were observed in October compared to November. Based on our results, this is likely due to more bare land at high latitudes in October compared to November. These results highlight that INP concentrations in the Arctic are likely sensitive to ice and snow cover at high latitudes. This is especially important since ice and snow cover at high latitudes are expected to decrease as temperatures continue to increase in the region.¹⁵

Related to the previous discussion, the combined results from the ammonium sulfate assay, the correlations between INPs and Al, and the particle dispersion modelling suggest that

Table 1 The correlation coefficients and p -values between the concentration of INPs at -16 °C and -22 °C and concentrations of Al, Na^+ , and Cl^- . Correlations that are statistically significant ($p < 0.05$) are bold

Tracer chemicals	Correlations between INPs and tracer chemicals ($n = 30$)			
	INPs at -16 °C		INPs at -22 °C	
	<i>R</i>	<i>p</i>	<i>R</i>	<i>p</i>
Al	0.58	3.4×10^{-4}	0.72	2.8×10^{-6}
Na^+	0.13	0.24	0.25	0.092
Cl^-	0.12	0.26	0.23	0.11



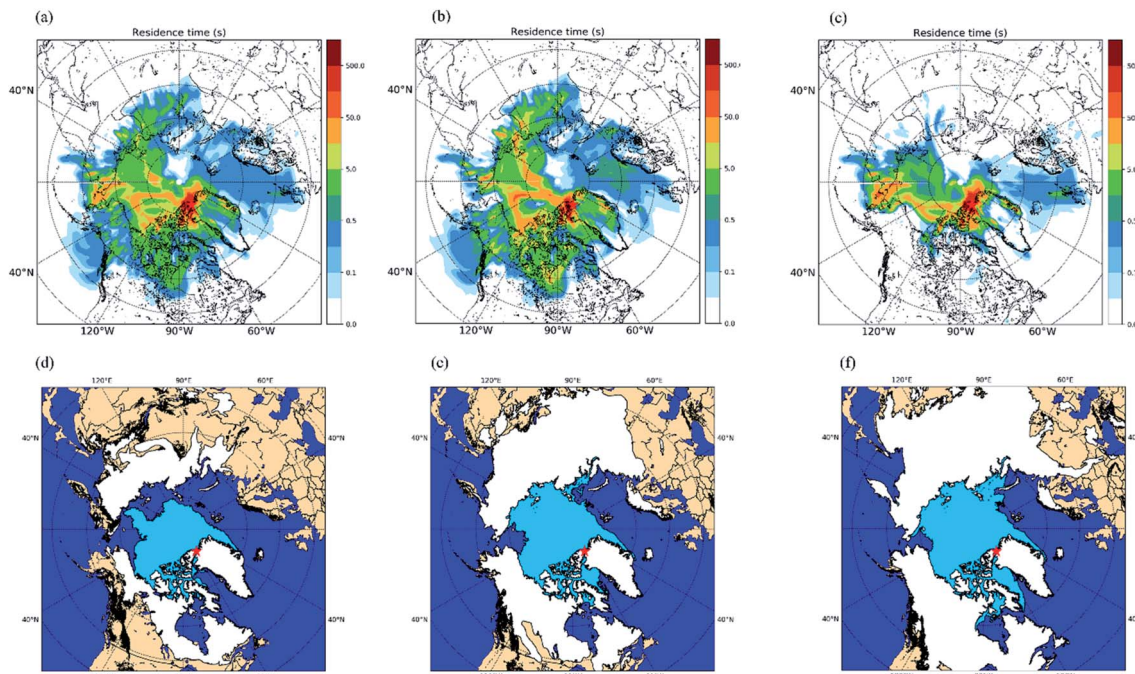


Fig. 5 Panel (a): the average footprint PES plots for all 30 samples collected in October and November. Panel (b): the average footprint PES plots for the samples collected in October. Panel (c): the average footprint PES plots for the samples collected in November. Panel (d): the map showing the surface coverage types on the first day of sampling (Oct-19). Panel (e): the map showing the surface coverage types at the midway point of sampling (Nov-03). Panel (f): the map showing the surface coverage types on the last day of sampling (Nov-17). In each panel, the sampling site is indicated by a red star. The surface coverage data was obtained from National Snow and Ice Data Center.

Table 2 The correlation coefficients and *p*-values between the concentration of INPs at $-16\text{ }^{\circ}\text{C}$ and $-22\text{ }^{\circ}\text{C}$ and the residence time of the airmass over different surface types within 0–100 m above the surface in the 7 days prior to sampling. Correlations that are statistically significant ($p < 0.05$) are bold

Surface coverage type	Correlations between INPs and residence time over different surface types ($n = 30$)			
	INPs at $-16\text{ }^{\circ}\text{C}$		INPs at $-22\text{ }^{\circ}\text{C}$	
	<i>R</i>	<i>p</i>	<i>R</i>	<i>p</i>
Land	0.49	0.003	0.53	0.0011
Sea	0.038	0.42	-0.08	0.33
Sea ice	-0.39	0.016	-0.42	0.01
Snow	0.1	0.3	-0.1	0.3

mineral dust from high latitudes is a significant source of INPs in the fall at Alert, Nunavut at $T \leq -20\text{ }^{\circ}\text{C}$. These findings are consistent with a recent study, Wex *et al.*,²⁶ which showed that mineral dust from high latitude sources such as the Hudson Bay area, eastern Greenland, or northwest continental Canada was an important contributor to the INP population of the Canadian Arctic marine boundary layer at $T \leq -15\text{ }^{\circ}\text{C}$ during the summer. These findings are also consistent with modelling studies that showed high-latitude mineral dust sources are a major contributor to total mineral dust aerosol population in the Arctic at the surface during the summer and fall.⁷⁶ As temperatures continue to increase in the Arctic region, concentrations

of mineral dust from high latitude sources are expected to increase.¹⁵ Hence, INP concentrations in the Arctic are also expected to increase, potentially resulting in an important climate feedback mechanism.

4. Summary and conclusions

In this study, we measured daily INP concentrations at Alert, a ground site in the Canadian High Arctic during October and November of 2018. The average INP concentrations were consistent with values from previous ground-based and ship-based INP measurements in the Arctic. The average INP concentrations fell within the INP concentration range reported by Petters and Wright⁷³ at a freezing temperature of $-16\text{ }^{\circ}\text{C}$ but were lower than this range at a freezing temperature of $-22\text{ }^{\circ}\text{C}$, suggesting that the INPs in the Arctic could be lower than those in mid-latitude continents at freezing temperatures of $-22\text{ }^{\circ}\text{C}$ and lower.

We used an ammonium sulfate assay and a heat assay to evaluate the importance of mineral dust INPs and biological INPs in the Arctic. The results from the ammonium sulfate assay suggest that mineral dust was an important component of the INP population for the October samples and November samples at $T \leq -21\text{ }^{\circ}\text{C}$ and $T \leq -20\text{ }^{\circ}\text{C}$, respectively. The results from the heat assay suggest that a large fraction of the INPs were likely biological for the October samples and November samples at $T \geq -21\text{ }^{\circ}\text{C}$ and $T \geq -16.5\text{ }^{\circ}\text{C}$, respectively.



We also measured the concentrations of Al, Na^+ , and Cl^- during the field campaign. At the freezing temperature of -22°C , we found statistically significant correlations between the concentrations of INPs and Al, consistent with mineral dust as an important component of the INP population. At the freezing temperature of -16°C , we observed a weaker but still statistically significant correlation between the concentrations of INPs and Al, although the results from the heat assay indicate that the majority of INPs at this freezing temperature were likely biological. This might be because the mineral dust INPs and biological INPs came from the same source, for example, soil dust particles. The contribution of soil dust particles to the total INP population could be explored further with a combination of a heat assay, ammonium sulfate assay, and H_2O_2 assay.^{33,77}

To help constrain the source regions of the INPs, FLEXPART was used to generate footprint PES plots. The footprint PES plots show the residence time of particles in the layer from 0 to 100 m in altitude during the previous 7 days. The footprint PES plots suggested the source regions of the INPs were likely at latitudes $>50^\circ\text{N}$. Using these PES plots and surface coverage data, we also calculated the residence time the air masses spent over each surface type (*i.e.* bare land, snow, open ocean, and sea ice). At the freezing temperatures of -16°C and -22°C , statistically significant positive correlations were found between the INP concentrations and the residence time the air masses spent over bare land, while statistically negative correlations were found between the INP concentrations and the residence time the air masses spent over sea ice. The results of particle dispersion modelling and a positive correlation between INP concentrations and Al suggest that the INPs were mostly from bare land at latitudes $>50^\circ\text{N}$. As temperatures in the Arctic continue to rise, bare land is expected to be exposed for longer periods of the year and the coverage extent of bare land is expected to increase.^{11,15} Hence, INP concentrations in the Arctic are also expected to increase, potentially resulting in an important climate feedback mechanism.

Conflicts of interest

There are no conflicts to declare.

Acknowledgements

The authors would like to acknowledge the funding provided by the Natural Sciences and Engineering Research Council of Canada (NSERC). We would also like to thank operators, students, and technicians for sample collection at Environment and Climate Change Canada Neil Trivett observatory at Alert and Canadian Force Services at Alert for maintaining the Alert station.

References

- 1 H. Morrison, G. De Boer, G. Feingold, J. Harrington, M. D. Shupe and K. Sulia, Resilience of persistent Arctic mixed-phase clouds, *Nat. Geosci.*, 2012, **5**, 11–17, DOI: 10.1038/ngeo1332.
- 2 M. D. Shupe, Clouds at arctic atmospheric observatories. Part II: thermodynamic phase characteristics, *J. Appl. Meteorol. Climatol.*, 2011, **50**(3), 645–661, DOI: 10.1175/2010JAMC2468.1.
- 3 I. Kudzotsa, T. J. V. Phillips and S. Dobbie, Effects of solid aerosols on partially glaciated clouds, *Q. J. R. Meteorol. Soc.*, 2018, **144**(717), 2634–2649, DOI: 10.1002/qj.3376.
- 4 A. Takeishi and T. Storelvmo, A Study of Enhanced Heterogeneous Ice Nucleation in Simulated Deep Convective Clouds Observed, *J. Geophys. Res.: Atmos.*, 2018, **123**(23), 13396–13420, DOI: 10.1029/2018JD028889.
- 5 U. Lohmann and J. Feichter, Global indirect aerosol effects: a review, *Atmos. Chem. Phys.*, 2005, **5**(3), 715–737, DOI: 10.5194/acp-5-715-2005.
- 6 P. J. De Mott, A. J. Prenni, X. Liu, *et al.*, Predicting global atmospheric ice nuclei distributions and their impacts on climate, *Proc. Natl. Acad. Sci. U. S. A.*, 2010, **107**(25), 11217–11222, DOI: 10.1073/pnas.0910818107.
- 7 T. Storelvmo, Aerosol Effects on Climate via Mixed-Phase and Ice Clouds, *Annu. Rev. Earth Planet. Sci.*, 2017, **45**, 199–222, DOI: 10.1146/annurev-earth-060115-012240.
- 8 U. Lohmann, F. Lüönd and F. Mahrt, *An Introduction to Clouds: From the Microscale to Climate*, Cambridge University Press, 2016, DOI: 10.1017/CBO9781139087513.
- 9 M. C. Serreze and J. A. Francis, The arctic amplification debate, *Clim. Change*, 2006, **76**, 241–264, DOI: 10.1007/s10584-005-9017-y.
- 10 IPCC Summary for Policymakers, in *Climate Change 2013: The Physical Science Basis. Contribution of Working Group I to the Fifth Assessment Report of the Intergovernmental Panel on Climate Change*, CEUR Workshop Proc., Published online, 2013, DOI: 10.1017/CBO9781107415324.004.
- 11 C. Derksen and R. Brown, Spring snow cover extent reductions in the 2008–2012 period exceeding climate model projections, *Geophys. Res. Lett.*, 2012, **39**(19), 1–6, DOI: 10.1029/2012GL053387.
- 12 Y. Tobe, K. Adachi, P. J. De Mott, *et al.*, Glacially sourced dust as a potentially significant source of ice nucleating particles, *Nat. Geosci.*, 2019, **12**(4), 253–258, DOI: 10.1038/s41561-019-0314-x.
- 13 J. M. Creamean, T. C. J. Hill, P. J. Demott, J. Uetake, S. Kreidenweis and T. A. Douglas, Thawing permafrost: an overlooked source of seeds for Arctic cloud formation, *Environ. Res. Lett.*, 2020, **15**(8), 1–10, DOI: 10.1088/1748-9326/ab87d3.
- 14 A. Sanchez-Marroquin, O. Arnalds, K. J. Baustian-Dorsi, *et al.*, Iceland is an episodic source of atmospheric ice-nucleating particles relevant for mixed-phase clouds, *Sci. Adv.*, 2020, **6**(26), 1–10, DOI: 10.1126/sciadv.aba8137.
- 15 J. E. Bullard, M. Baddock, T. Bradwell, *et al.*, High-latitude dust in the Earth system, *Rev. Geophys.*, 2016, **54**(2), 447–485, DOI: 10.1002/2016RG000518.
- 16 B. J. Murray, K. S. Carslaw and P. R. Field, Opinion: cloud-phase climate feedback and the importance of ice-nucleating particles, *Atmos. Chem. Phys.*, 2021, **21**(2), 665–679, DOI: 10.5194/acp-21-665-2021.



17 H. Wex, L. Huang, W. Zhang, *et al.*, Annual variability of ice-nucleating particle concentrations at different Arctic locations, *Atmos. Chem. Phys.*, 2019, **19**(7), 5293–5311, DOI: 10.5194/acp-19-5293-2019.

18 J. M. Creamean, R. M. Kirpes, K. A. Pratt, *et al.*, Marine and terrestrial influences on ice nucleating particles during continuous springtime measurements in an Arctic oilfield location, *Atmos. Chem. Phys.*, 2018, **18**(24), 18023–18042, DOI: 10.5194/acp-18-18023-2018.

19 A. G. Fountain and T. Ohtake, Concentrations and Source Areas of Ice Nuclei in the Alaskan Atmosphere, *J. Clim. Appl. Meteorol.*, 1985, **24**(4), 377–382, DOI: 10.1175/1520-0450(1985)024<0377:casaoi>2.0.co;2.

20 E. K. Bigg, Ice forming nuclei in the high Arctic, *Tellus B*, 1996, **48**(2), 223–233.

21 E. K. Bigg and C. Leck, Cloud-active particles over the central Arctic Ocean, *J. Geophys. Res., D: Atmos.*, 2001, **106**(23), 32155–32166, DOI: 10.1029/1999JD901152.

22 A. J. Prenni, P. J. Demott, D. C. Rogers, *et al.*, Ice nuclei characteristics from M-PACE and their relation to ice formation in clouds, *Tellus B*, 2009, **61**(2), 436–448, DOI: 10.1111/j.1600-0889.2009.00415.x.

23 F. Conen, E. Stopelli and L. Zimmermann, Clues that decaying leaves enrich Arctic air with ice nucleating particles, *Atmos. Environ.*, 2016, **129**, 91–94, DOI: 10.1016/j.atmosenv.2016.01.027.

24 M. Si, E. Evoy, J. Yun, *et al.*, Concentrations, composition, and sources of ice-nucleating particles in the Canadian High Arctic during spring 2016, *Atmos. Chem. Phys.*, 2019, **19**(5), 3007–3024, DOI: 10.5194/acp-2018-950.

25 R. H. Mason, M. Si, C. Chou, *et al.*, Size-resolved measurements of ice-nucleating particles at six locations in North America and one in Europe, *Atmos. Chem. Phys.*, 2016, **16**(3), 1637–1651, DOI: 10.5194/acp-16-1637-2016.

26 V. E. Irish, S. J. Hanna, M. D. Willis, *et al.*, Ice nucleating particles in the marine boundary layer in the Canadian Arctic during summer 2014, *Atmos. Chem. Phys.*, 2019, **19**(2), 1027–1039, DOI: 10.5194/acp-19-1027-2019.

27 T. Šant-Temkiv, R. Lange, D. Beddows, *et al.*, Biogenic Sources of Ice Nucleating Particles at the High Arctic Site Villum Research Station, *Environ. Sci. Technol.*, 2019, **53**(18), 10580–10590, DOI: 10.1021/acs.est.9b00991.

28 M. Hartmann, K. Adachi, O. Eppers, *et al.*, Wintertime Airborne Measurements of Ice Nucleating Particles in the High Arctic: A Hint to a Marine, Biogenic Source for Ice Nucleating Particles, *Geophys. Res. Lett.*, 2020, **47**(13), 1–11, DOI: 10.1029/2020GL087770.

29 M. Hartmann, X. Gong, S. Kecorius, *et al.*, Terrestrial or marine? – Indications towards the origin of Ice Nucleating Particles during melt season in the European Arctic up to 83.7 °N, *Atmos. Chem. Phys.*, 2021, **21**(15), 11613–11636, DOI: 10.5194/acp-21-11613-2021.

30 J. M. Creamean, J. N. Cross, R. Pickart, *et al.*, Ice Nucleating Particles Carried From Below a Phytoplankton Bloom to the Arctic Atmosphere, *Geophys. Res. Lett.*, 2019, **46**(14), 8572–8581, DOI: 10.1029/2019GL083039.

31 D. C. Rogers, P. J. Demott and S. M. Kreidenweis, Airborne measurements of tropospheric ice-nucleating aerosol particles in the Arctic spring, *J. Geophys. Res., D: Atmos.*, 2001, **106**(14), 15053–15063.

32 M. Kumai and K. E. Francis, Nuclei in Snow and Ice Crystals on the Greenland Ice Cap under Natural and Artificially Stimulated Conditions, *J. Atmos. Sci.*, 1962, **19**, 474–481.

33 T. C. J. Hill, P. J. Demott, Y. Tobo, *et al.*, Sources of organic ice nucleating particles in soils, *Atmos. Chem. Phys.*, 2016, **16**(11), 7195–7211, DOI: 10.5194/acp-16-7195-2016.

34 D. O'Sullivan, B. J. Murray, T. L. Malkin, *et al.*, Ice nucleation by fertile soil dusts: relative importance of mineral and biogenic components, *Atmos. Chem. Phys.*, 2014, **14**(4), 1853–1867, DOI: 10.5194/acp-14-1853-2014.

35 A. Ansmann, M. Tesche, P. Seifert, *et al.*, Evolution of the ice phase in tropical altocumulus: SAMUM lidar observations over Cape Verde, *J. Geophys. Res.: Atmos.*, 2009, **114**(17), 1–20, DOI: 10.1029/2008JD011659.

36 C. D. Westbrook and A. J. Illingworth, Evidence that ice forms primarily in supercooled liquid clouds at temperatures ≥ 27 °C, *Geophys. Res. Lett.*, 2011, **38**(14), 1–4, DOI: 10.1029/2011GL048021.

37 W. Richard Leaitch, L. M. Russell, J. Liu, *et al.*, Organic functional groups in the submicron aerosol at 82.5 °N, 62.5 °W from 2012 to 2014, *Atmos. Chem. Phys.*, 2018, **18**(5), 3269–3287, DOI: 10.5194/acp-18-3269-2018.

38 K. R. Spurny and J. J. P. Lodge, *Collection Efficiency Tables for Membrane Filters Used in the Sampling and Analysis of Aerosols and Hydrosols*, 1972, vol. 1, DOI: 10.5065/D6F769JJ.

39 P. J. DeMott, T. C. J. Hill, M. D. Petters, *et al.*, Comparative measurements of ambient atmospheric concentrations of ice nucleating particles using multiple immersion freezing methods and a continuous flow diffusion chamber, *Atmos. Chem. Phys.*, 2017, **17**(18), 11227–11245, DOI: 10.5194/acp-17-11227-2017.

40 T. F. Whale, B. J. Murray, D. O'Sullivan, *et al.*, A technique for quantifying heterogeneous ice nucleation in microlitre supercooled water droplets, *Atmos. Meas. Tech.*, 2015, **8**(6), 2437–2447, DOI: 10.5194/amt-8-2437-2015.

41 V. E. Irish, P. Elizondo, J. Chen, *et al.*, Ice-nucleating particles in Canadian Arctic sea-surface microlayer and bulk seawater, *Atmos. Chem. Phys.*, 2017, **17**(17), 10583–10595, DOI: 10.5194/acp-17-10583-2017.

42 V. E. Irish, S. J. Hanna, Y. Xi, *et al.*, Revisiting properties and concentrations of ice-nucleating particles in the sea surface microlayer and bulk seawater in the Canadian Arctic during summer, *Atmos. Chem. Phys.*, 2019, **19**(11), 7775–7787, DOI: 10.5194/acp-19-7775-2019.

43 Y. Xi, A. Mercier, C. Kuang, *et al.*, Concentrations and Properties of the Ice Nucleating Substances in Exudates from Antarctic Sea-Ice Diatoms, *Environ. Sci.: Processes Impacts*, 2021, **23**, 323–334, DOI: 10.1039/D0EM00398K.

44 G. Vali, Quantitative Evaluation of Experimental Results on the Heterogeneous Freezing Nucleation of Supercooled Liquids, *J. Atmos. Sci.*, 1971, **28**(3), 402–409, DOI: 10.1175/1520-0469(1971)028<0402:qoera>2.0.co;2.



45 T. Koop, B. Luo, U. M. Biermann, P. J. Crutzen and T. Peter, Freezing of $\text{HNO}_3/\text{H}_2\text{SO}_4/\text{H}_2\text{O}$ Solutions at Stratospheric Temperatures: Nucleation Statistics and Experiments, *J. Phys. Chem. A*, 1997, **101**(6), 1117–1133, DOI: 10.1021/jp9626531.

46 S. E. Worthy, A. Kumar, Y. Xi, *et al.*, The effect of $(\text{NH}_4)_2\text{SO}_4$ on the freezing properties of non-mineral dust ice nucleating substances of atmospheric relevance, *Atmos. Chem. Phys.*, 2021, **21**(19), 14631–14638, DOI: 10.5194/acp-21-14631-2021.

47 M. T. Reischel and G. Vali, Freezing Nucleation in Aqueous Electrolytes, *Tellus*, 1975, **27**(4), 414–427, DOI: 10.1111/j.2153-3490.1975.tb01692.x.

48 T. Whale, M. A. Holden, T. W. Wilson, D. O'Sullivan and B. J. Murray, The enhancement and suppression of immersion mode heterogeneous ice-nucleation by solutes, *Chem. Sci.*, 2018, **9**, 4142–4151, DOI: 10.1039/C7SC05421A.

49 A. Kumar, C. Marcolli, B. Luo and T. Peter, Ice nucleation activity of silicates and aluminosilicates in pure water and aqueous solutions – Part 1: the K-feldspar microcline, *Atmos. Chem. Phys.*, 2018, **18**(10), 7057–7079, DOI: 10.5194/acp-18-7057-2018.

50 A. Kumar, C. Marcolli and T. Peter, Ice nucleation activity of silicates and aluminosilicates in pure water and aqueous solutions-Part 2: quartz and amorphous silica, *Atmos. Chem. Phys.*, 2019, **19**(9), 6035–6058, DOI: 10.5194/acp-19-6035-2019.

51 A. Kumar, C. Marcolli and T. Peter, Ice nucleation activity of silicates and aluminosilicates in pure water and aqueous solutions-Part 3: aluminosilicates, *Atmos. Chem. Phys.*, 2019, **19**(9), 6059–6084, DOI: 10.5194/acp-19-6059-2019.

52 T. Koop and B. Zobrist, Parameterizations for ice nucleation in biological and atmospheric systems, *Phys. Chem. Chem. Phys.*, 2009, **11**(46), 10741–11064, DOI: 10.1039/b914289d.

53 L. A. Barrie and M. J. Barrie, Chemical components of lower tropospheric aerosols in the high arctic: six years of observations, *J. Atmos. Chem.*, 1990, **11**(3), 211–226, DOI: 10.1007/BF00118349.

54 L. A. Barrie and R. M. Hoff, Five Years of Air Chemistry Observations In The Canadian Arctic, *Atmos. Environ.*, 1985, **19**(12), 1995–2010.

55 P. Atkins and J. D. Paula, *Physical Chemistry*, W.H. Freeman, 9th edn, 2009.

56 E. Garcia, T. C. J. Hill, A. J. Prenni, P. J. DeMott, G. D. Franc and S. M. Kreidenweis, Biogenic ice nuclei in boundary layer air over two U.S. high plains agricultural regions, *J. Geophys. Res.: Atmos.*, 2012, **117**(17), 1–12, DOI: 10.1029/2012JD018343.

57 S. Pouleur, C. Richard, J. Martin and H. Antoun, Ice Nucleation Activity in *Fusarium acuminatum* and *Fusarium avenaceum*, *Appl. Environ. Microbiol.*, 1992, **58**(9), 2960–2964.

58 B. G. Pummer, C. Budke, S. Augustin-Bauditz, *et al.*, Ice nucleation by water-soluble macromolecules, *Atmos. Chem. Phys.*, 2015, **15**(8), 4077–4091, DOI: 10.5194/acp-15-4077-2015.

59 J. Fröhlich-Nowoisky, T. C. J. Hill, B. G. Pummer, P. Yordanova, G. D. Franc and U. Pöschl, Ice nucleation activity in the widespread soil fungus *Mortierella alpina*, *Biogeosciences*, 2015, **12**(4), 1057–1071, DOI: 10.5194/bg-12-1057-2015.

60 T. L. Kieft and T. Ruscetti, Characterization of biological ice nuclei from a lichen, *J. Bacteriol.*, 1990, **172**(6), 3519–3523, DOI: 10.1128/jb.172.6.3519-3523.1990.

61 B. C. Christner, R. Cai, C. E. Morris, *et al.*, Geographic, seasonal, and precipitation chemistry influence on the abundance and activity of biological ice nucleators in rain and snow, *Proc. Natl. Acad. Sci. U. S. A.*, 2008, **105**(48), 18854–18859, DOI: 10.1073/pnas.0809816105.

62 F. Conen, C. E. Morris, J. Leifeld, M. V. Yakutin and C. Alewell, Biological residues define the ice nucleation properties of soil dust, *Atmos. Chem. Phys.*, 2011, **11**(18), 9643–9648, DOI: 10.5194/acp-11-9643-2011.

63 L. Schütz and K. A. Rahn, Trace-element concentrations in erodible soils, *Atmos. Environ.*, 1982, **16**(1), 171–176, DOI: 10.1016/0004-6981(82)90324-9.

64 R. Balasubramanian, W. B. Qian, S. Decesari, M. C. Facchini and S. Fuzzi, Comprehensive characterization of PM2.5 aerosols in Singapore, *J. Geophys. Res., D: Atmos.*, 2003, **108**(16), 1–17.

65 W. C. Malm, J. F. Sisler, D. Huffman, R. A. Eldred and T. A. Cahill, Spatial and seasonal trends in particle concentration and optical extinction in the United States, *J. Geophys. Res., D: Atmos.*, 1994, **99**(1), 1347–1370, DOI: 10.1029/93JD02916.

66 P. K. Quinn, D. J. Coffman, T. S. Bates, *et al.*, Aerosol optical properties measured on board the Ronald H. Brown during ACE-Asia as a function of aerosol chemical composition and source region, *J. Geophys. Res.: Atmos.*, 2004, **109**(19), 1–28, DOI: 10.1029/2003JD004010.

67 P. K. Quinn, T. L. Miller, T. S. Bates, J. A. Ogren, E. Andrews and G. E. Shaw, A 3-year record of simultaneously measured aerosol chemical and optical properties at Barrow, Alaska, *J. Geophys. Res.: Atmos.*, 2002, **107**(11), AAC 8, DOI: 10.1029/2001jd001248.

68 J. D. Pfaff, *Methods 300.0: Determination of Inorganic Anions By Ion Chromatography*, 1993, DOI: 10.1016/b978-0-8155-1398-8.50022-7.

69 USEPA, *Method 300.7: Dissolved Sodium, Ammonium, Potassium, Magnesium, and Calcium in Wet Deposition by Chemical Suppressed Ion Chromatography*, 1986.

70 A. Stohl, Characteristics of atmospheric transport into the Arctic troposphere, *J. Geophys. Res.: Atmos.*, 2006, **111**(11), 1–17, DOI: 10.1029/2005JD006888.

71 H. Goldstein and M. J. R. Healy, The Graphical Presentation of a Collection of Means, *J. R. Stat. Soc.*, 2009, **158**(1), 175–177, DOI: 10.2307/2983411.

72 L. F. Radke, P. V. Hobbs and J. E. Pinnons, Observations of Cloud Condensation Nuclei, Sodium-Containing Particles, Ice Nuclei and the Light-Scattering Coefficient Near Barrow, Alaska, *J. Appl. Meteorol.*, 1976, **15**(9), 982–995, DOI: 10.1175/1520-0450(1976)015<0982:oocns>2.0.co;2.



73 M. D. Petters and T. P. Wright, Revisiting ice nucleation from precipitation samples, *Geophys. Res. Lett.*, 2015, **42**(20), 8758–8766, DOI: 10.1002/2015GL065733.

74 D. O'Sullivan, B. J. Murray, J. F. Ross, *et al.*, The relevance of nanoscale biological fragments for ice nucleation in clouds, *Sci. Rep.*, 2015, **5**, 1–7, DOI: 10.1038/srep08082.

75 D. O'Sullivan, B. J. Murray, J. F. Ross and M. E. Webb, The adsorption of fungal ice-nucleating proteins on mineral dusts: A terrestrial reservoir of atmospheric ice-nucleating particles, *Atmos. Chem. Phys.*, 2016, **16**(12), 7879–7887, DOI: 10.5194/acp-16-7879-2016.

76 C. D. Groot Zwaftink, H. Grythe, H. Skov and A. Stohl, Substantial contribution of northern high-latitude sources to mineral dust in the Arctic, *J. Geophys. Res.*, 2016, **121**(22), 678–697, DOI: 10.1002/2016JD025482.

77 R. J. Perkins, S. M. Gillette, T. C. J. Hill and P. J. Demott, The Labile Nature of Ice Nucleation by Arizona Test Dust, *ACS Earth Space Chem.*, 2020, **4**(1), 133–141, DOI: 10.1021/acsearthspacechem.9b00304.

